Testing and integrating the laser system of ARGOS: The Ground Layer Adaptive Optics for LBT

C. Loose[a], S. Rabien[a], L. Barl[a], J. Borelli[b], M. Deysenroth[a], W. Gaessler[b], H. Gemperlein[a], M. Honsberg[a], M. Kulas[b], R. Lederer[a], W. Raab[a], G. Rahmer[c], J. Ziegleder[a]

[a]Max-Planck-Institut für Extraterrestrische Physik, Garching, Germany
[b]Max-Planck-Institut für Astronomie, Heidelberg, Germany
[c]Large Binocular Telescope, Tucson, Arizona, USA

ABSTRACT

The Laser Guide Star facility ARGOS will provide Ground Layer Adaptive Optics to the Large Binocular Telescope (LBT). The system operates three pulsed laser beacons above each of the two primary mirrors, which are Rayleigh scattered in 12 km height. This enables correction over a wide field of view, using the adaptive secondary mirror of the LBT. The ARGOS laser system is designed around commercially available, pulsed Nd:YAG lasers working at 532 nm. In preparation for a successful commissioning, it is important to ascertain that the specifications are met for every component of the laser system. The testing of assembled, optical subsystems is likewise necessary. In particular it is required to confirm a high output power, beam quality and pulse stability of the beacons. In a second step, the integrated laser system along with its electronic cabinets are installed on a telescope simulator. This unit is capable of carrying the whole assembly and can be tilted to imitate working conditions at the LBT. It allows alignment and functionality testing of the entire system, ensuring that flexure compensation and system diagnosis work properly in different orientations.

Keywords: Laser Guide Stars, Ground Layer Adaptive Optics, Large Binocular Telescope, System Testing

1. INTRODUCTION

The Large Binocular Telescope on Mount Graham in Arizona features two co-mounted 8.4 m primary mirrors. The First Light Adaptive Optics System came online in 2010 working with one of the two deformable secondaries. Using natural star guiding, Strehl ratios of 60%–80% were achieved in the H band. The Advanced Rayleigh Ground Layer Adaptive Optics System, ARGOS,[1,2] will equip the Large Binocular Telescope with multiple laser guide stars to provide extended-field correction of the strong atmospheric ground layer, at almost full sky coverage.

ARGOS is designed to enhance the capabilities of the twin LUCI instruments.[3,4] One per LBT eye, they offer imaging, long-slit and multi-object spectroscopy in the near-infrared z, J, H and K bands over $4' \times 4'$ wide fields of view. This makes LUCI a preferred and efficient tool for the study of many targets in one observation. Homogeneity of the turbulence compensation is therefore an imperative requirement for the associated Adaptive Optics concept. The Ground-Layer Adaptive Optics provided by ARGOS is expected to concentrate the PSF by a factor of 1.5–3, depending on the observed band and seeing conditions.[1,5] This will, on the one hand, enable observations at a higher resolution, improving the sensitivity to unresolved sources and mitigating effects of crowding. At the same time, the ensquared energy for a $0.25''$ slit will be augmented by a similar factor of about 1.5–3. The resulting improvement of observing efficiency is considerable: The same signal to noise ratio can be obtained in as little as one-ninth the integration time.

Two laser guide star (LGS) constellations are positioned at the outer edges of the LUCI fields of view. Each is composed of three powerful 18 W laser beams projected into a triangular pattern with nominal $2'$ radius at 12 km height. The beacon constellations are formed in a laser system mounted on a platform attached to the telescope support structure between the primary mirrors, which triggers the lasers to emit synchronous pulses of ~ 40 nm width at a 10 kHz repetition frequency. The beams are positioned individually onto a common pupil mirror,

Correspondence: e-mail cloose@mpe.mpg.de

Adaptive Optics Systems III, edited by Brent L. Ellerbroek, Enrico Marchetti, Jean-Pierre Véran, Proc. of SPIE Vol. 8447, 84474I · © 2012 SPIE · CCC code: 0277-786/12/$18 · doi: 10.1117/12.927101

which is followed by a set of small lenses mounted on a z-stage close to the exit window of the laser system box. Optically, these comprise the low end of the launch telescope, expanding the beams 50-fold to roughly 30 cm diameter each while they propagate upwards in a protective dust tube. An aspheric lens of 400 mm diameter focusses the guide stars to the targeted altitude of 12 km. Finally, the beams are folded by a large, flat mirror towards the back of the adaptive secondary mirror, from where they are launched on-axis by a second large flat. The laser system foresees space for fourth laser, and mounts for associated, additional optics. Since all common mirror coatings were chosen with a high reflectivity both at 532 nm and 589 nm, ARGOS can be equipped with an additional sodium guide star with relatively little effort, an upgrade aiming at on-axis diffraction limited performance.

The laser return signal, Rayleigh scattered back towards the telescope by the atmosphere, is reflected from a large dichroic window installed in front of LUCI. Wavelengths on the red side of 600 nm are transmitted; while the infrared light is used for science by LUCI, the transmitted optical component drives the natural guide star tip-tilt tracker and truth sensing, both performed inside the acquisition, guiding and wavefront-sensing unit (AGW) installed on the rotator structure in front of the instrument. The reflected, green light is diverted by a pick-off mirror to the LGS wavefront sensing unit installed on a support platform beside the bent Gregorian focal station of LUCI. Pockels cells range gate the backscattered light that reaches the wavefront sensor to within 300 m of the beacon target height.[6] A large Shack-Hartmann lenslet array samples the three beacons with 15 subapertures across each pupil, and projects the images onto one fast, low-noise 264×264 px CCD. The averaged measurements of all LGS are used to extract a command correcting for ground layer turbulence, which is then applied by the adaptive secondary mirrors.

The initial stage of the ARGOS facility, in particular the two laser systems, will commence commissioning end of this year. This paper describes these systems and their components as they have been integrated and reports on their verification and characterization. Assembly is next to finished and testing is ongoing with final results expected before the end of this summer.

2. LASER SYSTEM

For a summary of the ARGOS project status please refer to Gaessler et al.[2] in these proceedings. Here we will focus on the laser system developed at the Max Planck Institute for Extraterrestrial Physics in Garching, Germany. The two laser systems, one for each of the LBT sides, are referred to as the DX (right) and SX (left) sides as seen from in front of the telescope, from the Latin dexter and sinister. Figure 1 illustrates the design of the system as described below.

2.1 Laser System Design

Each system is encased in a rigid, steel-framed box covered by insulating panels, and is temperature controlled just as the two cabinets are which supply the electronic and cooling system required for their operation. The inner design of the systems is identical. Three laser heads are mounted parallel to each other in a square configuration that leaves one space for a future upgrade. They are frequency-doubled Nd:YAG lasers of the NANIO series from *InnoLas*, rated at a nominal 18 W output power each and operating at 532 nm with a nominal pulse repetition rate of 10 kHz.

The beams emitted from the lasers are immediately expanded and recollimated by a set of Galilean 6× beam expanders mounted directly on the front plate of the laser heads. That way each beam is about 6 mm wide in $1/e^2$ while propagating through the system, reducing the beacon susceptibility to optical surface errors as well as the energy surface density on the optical components. The pre-expanders protrude from a partition wall which fashions the interface between the laser compartment and that part of the laser box containing the optics, which is thereby isolated against particles—as well as 'tiny life-forms'.

The plane of polarization of each beam is adjusted parallel to the LUCI optical axis in order to match the Pockels cell range-gating the wavefront sensor, by crystalline $\lambda/2$ waveplates installed in a z-rotating mount. Next, on the same intermediate wall, two tip-tilt mirrors per beam are arranged in periscope style. This allows a shift in beam position to form the beacon constellation, while retaining the direction of propagation along the optical axis of the system. A fast photodiode installed behind each first periscope mirror uses the small fraction

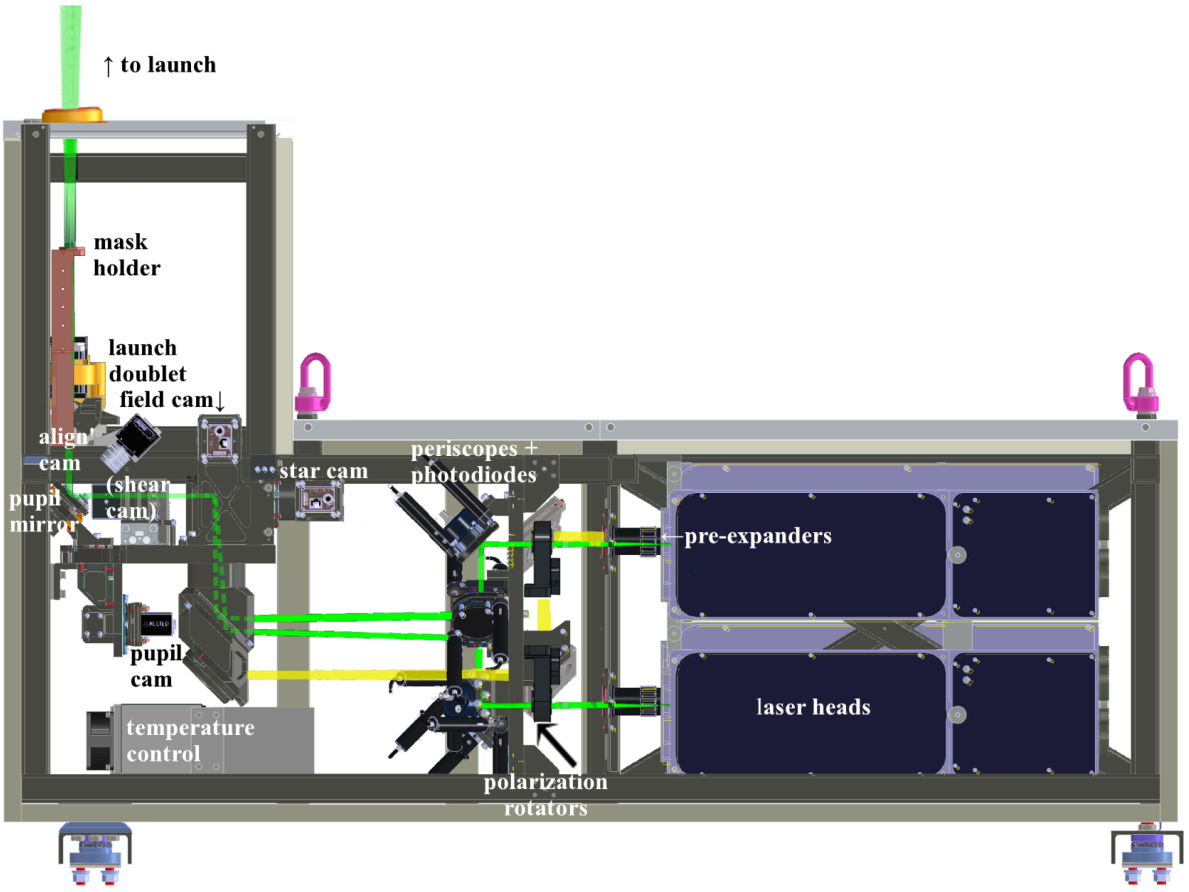

Figure 1. Mechanical design of the laser system with the beams traced in green, dashed where direct view is obstructed. The 589 nm upgrade path is indicated in yellow and important subsystems are labeled for clarity.
Three 532 nm high-power lasers are installed in the right-hand compartment of the box, each 59 cm long, with space for a sodium guide laser of similar dimensions. The laser beams are immediately pre-expanded and adjusted in polarization—with reference to the system exit. Two tip-tilt periscope mirrors are responsible for the active positioning of each of the laser beacons, compensating for system internal flexure. Upstream cameras use light transmitted through two folding mirrors to image the pupil and focal planes, a diagnostic shearing plate, the pupil mirror, or a wide field of the sky imaged backwards through the beam launch configuration. The laser beams are steered onto the pupil mirror, from where they are directed upwards through a beam-expanding set of lenses into the launch telescope.

of light transmitted to continuously detect the laser pulses. A central hub of three elliptical alignment mirrors steers the beams into a single path of common optical components. The beams are folded by two flat mirrors onto the pupil mirror which directs the constellation upwards through the launch telescope. It is mounted on a piezo-operated, fast-response tip-tilt stage and is able to quickly compensate, for the entire constellation, for vibration of the laser system. A compressed-air operated shutter is installed in front of the pupil mirror. It has a mirror mounted to its back side which reflects the laser beams onto a powermeter, and so allows to check the power output when the shutter is closed.

An interlock system controls the release of this shutter, preventing or stopping light emission unless all attached systems confirm save operation. Conditions are the presence of a heartbeat signal from the aircraft avoidance system, and the absence of an aircraft approach warning from spotter remote controls. A release of the compressed air shutter is signaled by a pre-warning and warning light sequence as well as a loud buzzer sound inside the dome. Laser system cover, service lockout and emergency switches additionally override operator commands to fire the lasers at all, using internal shutters in the laser heads to ensure personel safety.

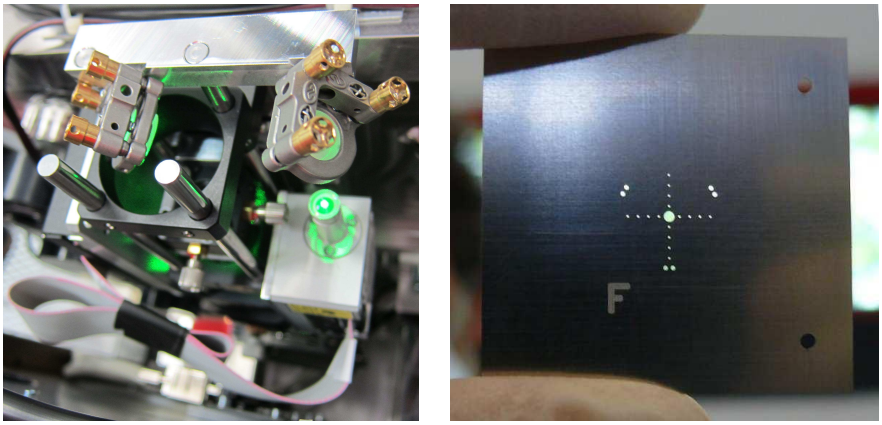

Figure 2. The left image shows the *alignment laser assembly* with its focus stage, as seen from the back of the laser box, i.e. so that the pupil mirror lies in the forward direction. The focal alignment mask is shown on the right, featuring a large central hole and a smaller cross-hair pattern for centering; the outer holes marking the nominal constellation positions are in duplicate so that one mask can be used to align both the DX and SX system. The 'F' engraving can be illuminated from above to easily identify the masks orientation on the camera.

2.2 Diagnostic Cameras

Five diagnostic cameras with according re-imaging optics are incorporated in the laser system. We use GC1350 CCD by *AVT/prosilica* with 1360 px × 1024 px resolution. None of the integrated cameras is located in the primary beam path:

- The *pupil imager* is installed behind the lower folding mirror. A set of lenses images the pupil of each beam individually onto a single camera, using the small fraction of light transmitted.
- The *field imager* is similarly situated behind the upper folding mirror and images the focal plane with a small defocus, allowing for well-resolved images of the constellation of laser beams.
- The *star camera* is also installed behind the upper folding mirror. However, it faces the pupil mirror instead of the lasers and thus images a $6' \times 6'$ wide field of sky used to align the LGS constellation with the LBT optical axis. A 30 nm narrow band around 650 nm avoids the reflecting wavelengths of the mirror coating and allows imaging through the launch telescope.
- The *shear camera* uses light reflected from a window in front of the powermeter, illuminated when the shutter is closed. It monitors a shear plate used to check the beam collimation before the pupil mirror.
- The *alignment camera* is installed off-axis and directly observes light scattered from the entire pupil mirror.
- Additionally, there is the *test camera*, which is part of the test setup described in Section 2.4. It can be installed temporarily on top of the laser system to access its exit beam.

All except the star camera are equipped with neutral density filters because the high-power beam residuals are still far too bright for their sensitivity. The pupil and field camera images are used to drive a flexure-compensating loop for each of the periscope pairs, with the task of controlling each beam position against drifts and thus maintain the constellation.

2.3 Alignment Setup and Concept

The alignment concept is based on a dedicated, central 532 nm laser with less than 100 mW output, that delivers a beam with an $M^2 < 1.2$ just as the high-power lasers. It is used to mark the center of the constellation, as defined by the optical axis through the pupil mirror center and the center of a mask introduced above at the focus. A vertical beam is used as mask holder, it is indicated in red in Fig. 1. It provides several positions above the pupil mirror where an alignment mask can be installed, in particular in the focal plane above the focus stage holding the launch telescope beam expanding lens doublet.

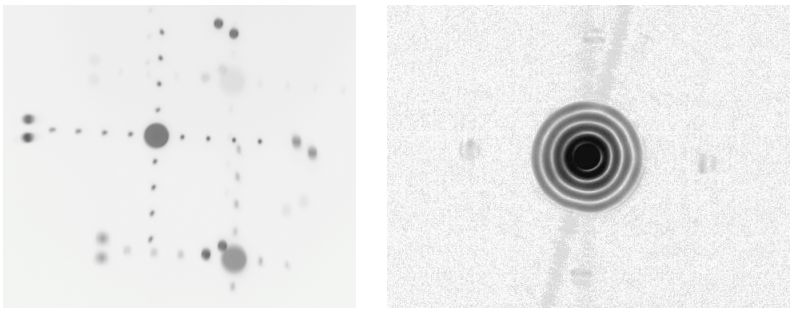

Figure 3. These images taken with the test camera serve to illustrate the *alignment process* defining an internal optical axis using the alignment laser. They show only part of the full camera image and were inverted and scaled to enhance details. The *left* image shows the alignment laser shining through the central hole. It was used to determine if the alignment laser had been well centered. For the image on the *right*, the alignment focus mask was illuminated homogeneously from the back with a lamp. Two ghost images origin from back-reflections from windows used in the test setup.

A compact assembly providing the alignment laser beam is installed at the back side of the periscope intermediate wall and folded by a small, central mirror onto the common optical axis of the high-power laser beams. It is equipped with a set of lenses, one of which can be moved along a z-stage as depicted in Fig. 2. This way, the beam from the alignment laser can be either focussed around the pupil mirror, or collimated. To ensure that this does not change the alignment beam axis, the assembly is aligned in itself prior to integration into the laser system using two flat folding mirrors.

Internal Alignment Procedure

A first step of internal alignment is the definition of the central optical axis. Using the alignment camera to monitor the pupil mirror, which is set to its nominal zero position at actuator mid-range, the focussed alignment beam is steered to its center with an accuracy of $\sim 50\,\mu$m. While the launch doublet is not installed, the pupil mirror is then adjusted to feed the beam centrally through the focal mask, which is re-imaged by the test camera. Two masks with different hole sizes are to be used consecutively, centering first on a 0.5 mm, then a 100 µm central hole. The camera images shown in Fig. 3 were taken during the alignment process.

Collimating the alignment beam, the launch telescope lens doublet is shifted until the marked constellation center on the test camera is hit. Its tilt is then corrected by overlaying the back-reflection onto the uplink beam. The alignment is iterated if movements along the launch z-stage displace the beam on the test camera.

Constellation Alignment Procedure

Secondly, the constellation is arranged around this central axis. Low-power, pencil lasers are installed in mounts so as to function as dummies for the high-power heads, which allows save operation of the unaligned system. With the periscope mirrors set to mid-range, the elliptical hub mirrors are adjusted to center the beams on the pupil mirror, monitored by the alignment camera. The constellation positions on the test camera are marked by illuminating the 100 µm hole focal mask from the back with a lamp. The pen laser beams are then steered to these positions using the periscope mirrors, while iteratively maintaining the beam position on the pupil mirror. When this is done, the beam positions on pupil and field camera are noted.

The high-power laser heads are then installed and the beam locations on the pupil mirror and field mask re-checked at low power. After the beam positions on the pupil and field camera are confirmed, they define the nominal points for the flexure compensation loop driving the periscopes.

2.4 Auxiliary Test Setups

Exit Beam Test Setup

An additional diagnostic setup was designed that allows access to the beam exiting the laser system. All its components are installed on a breadboard, which can be firmly clamped directly onto the frame top above pupil mirror as illustrated in Fig. 4.

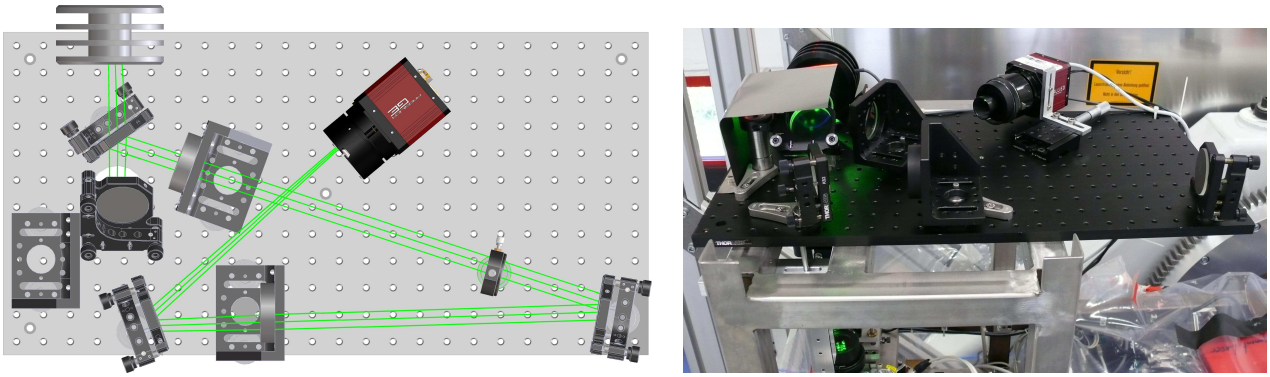

Figure 4. The *test setup* with a high-resolution CCD camera and an additional powermeter can be installed on top of either laser system to access its exit beam. Lenses are used to observe a slightly magnified image of the focal plane, in particular to observe the alignment masks. On the right, the setup is seen during a first alignment run; the triangular 'constellation' of three test beams can be seen on the entrance window, coming from the launch doublet just visible below.

Two 50 mm-diameter achromats project a slightly magnified image of the focal plane onto a 4008 px × 2672 px large CCD, a GE4000 by *AVT/Prosilica*. Like this, the setup is able to image the whole focal plane mask, including the orientation mark if illuminated from above. The plate scale is roughly 3.3 µm/px, so the masks small holes are well sampled resolved.

The camera uses only a negligible fraction of the light, which is reflected from a window in front of a calibrated powermeter. The total power exiting the laser system can thus be measured conveniently.

M^2 Beam Characterization Setup

The diagnostic cameras do not allow for a validation of the lasers nominal, single-mode operation close to the diffraction limit—although the field camera image would show a considerable degradation in beam shape. It should be possible, however, to check the beam quality in detail without dismounting the laser, as would be required e.g. if a laser beacon behaves suspiciously or at intermittent health checks. This necessity has been stressed since we identified several factors which may cause the laser beam to degrade in quality.

For this reason, another small setup will be devised, dedicated to beam characterization with the M^2 meter by *metrolux* that has been used in our laboratory tests. This instruments allows the setup to remain handy, i.e. compact and rigid so it can be stored and re-installed with as little effort as possible. It already implements automated filter wheels and a motorized focussing lens.

The system exit beam can be extracted below the launch doublet using a mirror mounted on a small stage, by removing the insulation panel from the back side of the upper frame. This arrangement will serve the 4D interferometer used to align the launch telescope. Since this will be installed only temporarily during commissioning, its mount attached to the top cover of the lower section laser box would be a convenient position for the beam characterization setup.

2.5 Integration Status and Telescope Simulator

System assembly begun early this year, after the construction of the welded steel frames of the two laser boxes. It was mainly the progress of the detailed design and manufacture of the laser systems mechanical components which set the pace after then. As of now, the assembly is virtually finished except for few components which are not pre-requisite to operation. Namely, the outer cover providing both systems with protection against particle intrusion and thermal insulation, consisting of rubber grommets and vacuum panels, are just now being assembled and installed. Both laser systems are equipped with all optics, motorized and diagnostic subsystems and an pre-aligned alignment laser assembly. Both have been operated using the ARGOS software.

The electronic and cooling systems of one laser box fills two 19-inch racks. At LBT, one of these racks will be standing right behind the back side of the laser system, i.e. on the far side of the beam exit, while the other will be installed on a supply platform below and slightly offset from the corresponding rack on the laser platform.

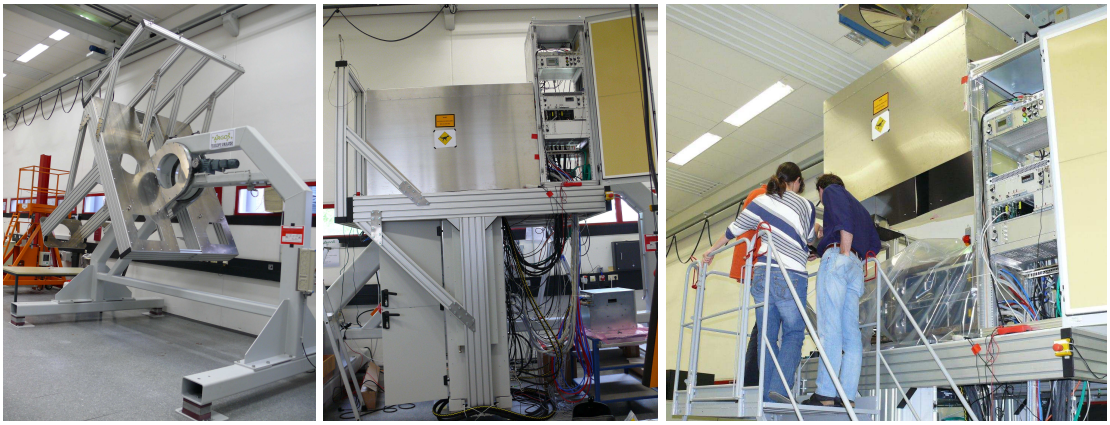

Figure 5. The *telescope simulator* can carry both laser systems and the four racks required for their operation. The simulator is equipped with a powerful motor that allows the entire platform—including the downwards extension carrying the lower racks—to be tilted to the right. This setting simulates the strains at LBT, when the telescope and therefore all systems installed on are pointed far from the nominal Zenith position towards lower elevation.

Both platforms are attached to the telescope structure and will therefore tilt backwards with increasing Zenith distance of the LBT, by as much as 90° when the telescope points at the horizon e.g. for maintenance access.

The 'telescope simulator' is designed to mimic this environment. As shown in Fig. 5, it consists of a platform large enough to mount both laser systems and the two laser racks simultaneously, with downward extensions for the supply racks. It is motorized and can be tilted back to allow full-system verification tests at varying inclinations.

Since the laser boxes are not yet equipped with covers, only one is currently installed on the telescope simulator, along with the electronic cabinets that operate it. An simple aluminum cover is used to encase a laser system, which allows relatively quick access without compromising safety during high-power operation. The DX laser system started operation in this fashion in May. The experience gained during this testing period benefits both hardware and software reliability.

3. COMPONENT VERIFICATION AND SYSTEM TESTING

As for any complex system, functional tests of the single components, be they mechanical or pre-assembled subsystems, are the prerequisite to assembly of the ARGOS laser system. The confirmation of any particular specifications as well as conformity with interacting systems and operating software are the goals, the majority of which can be tested 'stand-alone' in the laboratory environment. We will focus on the characterization of the seven interchangeable laser heads, including one spare as drop-in replacement. They are the core components of the laser system and their performance sets the standard for the ARGOS facility.

The second part will detail tests on the integrated system. Experience in operating the full system strongly benefits its robustness on the telescope, since any malfunctions can be isolated and resolved more easily and therefore less time consuming in the testing environment. The validation of the system specifications is ongoing.

3.1 Laser Performance

Seven commercial laser heads, including one spare, were tested and characterized in the laboratory. They are frequency-doubled, pulsed Nd:YAGs of the NANIO 18 W series by *InnoLas*, which were operated at pulse repetition frequencies between 5 kHz and 30 kHz, with a strong emphasis on the performance at nominal 10 kHz. The lasers can be operated stand-alone conveniently using interchangeable controllers, or accessed using the ARGOS software interface. Three water–water chillers were acquired, again including one spare, which can each supply three heads with cooling water at constant 20° C. Please refer to Section 3.2 for pulse properties and beam polarization.

Output Power
The laser output power responds to the current applied to the pumping diodes. For all heads, this relation was characterized for pulse repetition frequencies ranging from 5 kHz to 30 kHz. The power shows an overall increase with applied current up to a critical point, beyond which it eventually drops quite rapidly. Operation beyond this current should be avoided. The working point is defined for operation at 10 kHz, at the lowest current where the nominal power of 18 W is achieved; it is individual to each laser head. Several heads did achieve higher output powers of up to 20 W if driven at a current beyond the working point. However, at this setting, each laser delivers optimal beam quality—not necessarily at higher currents.

The lasers require a warm-up time of ~ 15 min, after which they operate very stable. The working point power has been monitored over day-long periods and showed only minimum variation of less than $\pm 5\%$, which corresponds to the accuracy of the powermeter used for the characterization. Some heads react rather sensitively to an increase of the cooling water temperature, nominally set to 20°C and controlled by the chillers to within a range of ± 0.1°C. The strongest response was found to be a decrease in power by roughly 1 W when the cooling temperature was increased by 1°C.

Beam Quality
The spatial mode was investigated with a stand-alone CCD camera as well as with an M^2 meter by *metrolux*. The laser beams are < 1 mm in $1/e^2$ diameter, with a divergence well below 1 mrad. Clean, single-lobed beam profiles were observed, which fit well to a Gaussian. The beams of a few heads exhibit a certain ellipticity, in the order of but within the requirement of >80 % beam roundness.

The M^2 was measured in order to confirm single-mode TEM_{00} behaviour close to the diffraction limit, where the dimensionless parameter would be equal to 1. The requirement is an M^2 <1.2, which means that the area of the focus spot is larger than that of a diffraction limited laser by this factor. The beam quality is sensitive to changes in operating current, although the degree varies from head to head. So if a laser is to be operated off the working point, it is necessary to check the beam quality with this setting. Relatively small changes that may improve the power output, can decrease the M^2 to 1.3–1.5.

Performance and Reliability
Our lasers have been acquired almost three years ago and underwent service in the past to exchange components. Some heads have been powered for a few hundred hours. Although wear-out is not expected to start affecting performance before roughly a thousand hours of operation, we encountered several incidents where the output power and beam quality degraded below out specifications. The manufacturer proved highly cooperative in the process of tracing the different causes and in resolving them.

This experience stresses the importance of regular tests of each laser head before shipping the system to LBT, to verify steadily high performance over several months. With the DX system in full operation on the telescope simulator and the SX system also ready to be put in full operation, this is becoming a routine task. In addition, the performance of all lasers is to be verified under varying angles of tilt on the telescope simulator. This will be done once the laser systems insulating cover is installed, so that the temperature in the laser system is well-controlled at the time and turbulences still present now are reduced. The lasers are mounted on their left or right sides, depending on the position in the laser system, i.e. they are permanently rotated around their longitudinal axis by $\pm 90°$. Additionally, they must operate according to specifications when the telescope points at Zenith distances of 60°, which means the lasers point upwards, and tolerate perpendicular positioning when the telescope points at Horizon.

3.2 Integrated System Tests

While the mechanical components of the laser system were being manufactured, a mock-up of one laser system beam path was setup on an optical bench in the laboratory. It is depicted and detailed in Fig. 6. This allowed using the ARGOS operation software—which is being developed at Max-Planck-Institute for Astronomy in Heidelberg, Germany—to be tested in interaction with the multitude of integrated hardware before the actual laser system could be assembled. The basic commanding of the laser controller and motorized elements, from the periscope actuators to the shutter stage, was confirmed as well as read-out of the diagnostic elements, i.e. photodiode, powermeter and the three installed cameras. In the process, the setup was used to check test scripts.

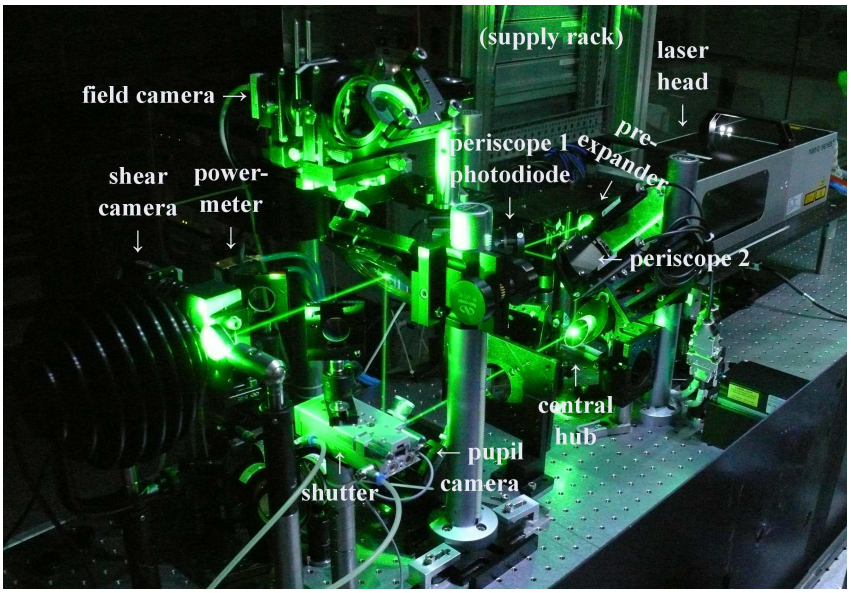

Figure 6. Laboratory installation describing the optical *path of one laser* through laser system. The beam propagates from the laser head on the left side to the powermeter on the right, which replaces the pupil mirror of the laser system. The interaction of the operating software with all installed hardware components was tested, commanding the laser head, the shutter and the periscope motors, and reading out the photodiode and powermeter measurements as well as the camera images. A drift compensation loop was developed and tested, which uses the periscopes to stabilize the beam position on the pupil and field camera against flexure.

In particular, the flexure compensation loop was tested, which iteratively compensates for drifts in beam position on the focal and pupil imager cameras using one periscope for correcting one plane.

Meanwhile, the system assembly has progressed to an almost final stage. The alignment of both laser systems is ongoing as the early images in Fig. 3 demonstrate. One system is mounted on the telescope simulator and first tests on the fully integrated systems are being performed. The following paragraphs detail some of these measurements.

System Throughput

The pencil lasers foreseen for the alignment of the constellation were in a first instance used to measure the system throughput. Three of the $\sim 5\,\mathrm{mW}$ 532 nm lasers and one $\sim 100\,\mathrm{mW}$ laser at 589 nm were installed in place of the high-power green and upgrade lasers, positioning their beams roughly onto the foreseen beam paths. The ratio of the power picked up with a hand-held powermeter above the pupil mirror, to the power measured directly at the pen laser apertures, was determined. This measures the optical transmission of the combination of all optical components, except the pre-expanders and the launch doublet, which were not installed during the test. The 95 % total transmission requirement is confirmed for all six green paths, as well as for both upgrade paths.

Polarization Rotation

ARGOS uses Pockels cells for range gating of the LGS return signal, which operate by rotating the polarization. They are equipped with up- and downstream polarizers that filter any component that is not parallel to the LUCI optical axis. The lasers are required to be highly linearly polarized, to a degree of $> 100:1$, parallel to their base plates. Rayleigh scattering conserves the polarization. To match the plane of polarization of the laser beacons with the Pockels cells, the laser beams should leave the laser system polarized along the LUCI optical axis.

To this aim, a polarizer is introduced into the beam above the pupil mirror, which is oriented to safely less than 5° of the LUCI optical axis, which confines an angle of 25.9° with the front of the laser system. One laser at a time is operated at a low power of $\sim 1\,\mathrm{W}$, in order to remain within the polarizers damage threshold. The test setup powermeter on top of the system is used to measure the fraction of light transmitted through the

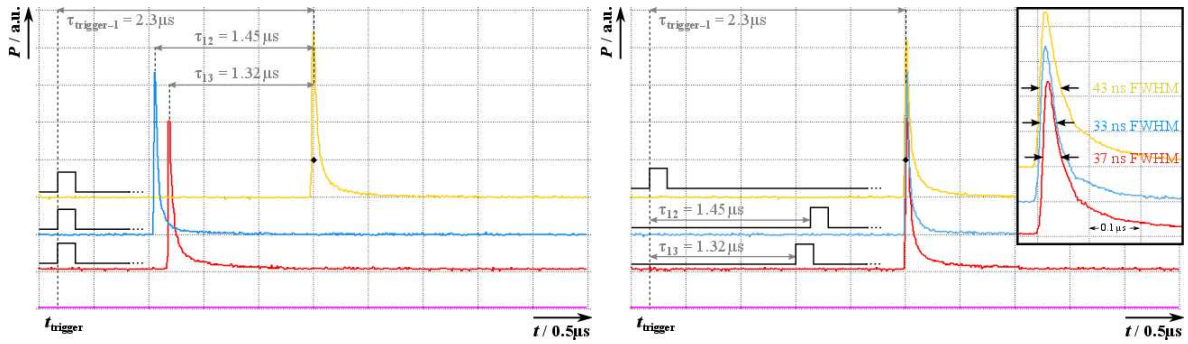

Figure 7. Visualization of the ARGOS high-power *laser pulses* at 10 kHz repetition frequency. The pulses are detected with photodiodes and read out by an oscilloscope which can be conveniently accessed with the operation software. By applying delays to the triggering signals from the pulse generator, synchronicity of the pulses is achieved.
The diode signals were rescaled to the same magnitude and offset in power to allow easy comparison of the pulse shapes. The delays τ are indicated, and the stylized trigger signals added for the sake of illustration. The upper right inlay shows the pulses in more detail, using a finer timescale.

polarizer, while the beams polarization plane is rotated using the $\lambda/2$ wave plates installed directly after the pre-expanders. The results neatly fit the expected $\sin^2$, and the wave-plate rotators are adjusted for maximum transmission.

One of the three lasers for which this procedure performed shows a residual, non-zero minimum intensity that cannot be accounted for by power measurement uncertainties. We find this apparently non-linearly polarized component to be on the order of $\sim 10\%$. That part of the beacon power is essentially lost to the LGS wavefront sensor. We are currently investigating possible causes for this measurement.

Trigger Delay

Although our lasers can be triggered internally by their native controlling system, this is not sufficient for the coordinated operation in an integrated system. The trigger-to-pulse delay is an individual property of each laser head, but constant over time. This means that in order to fire the lasers synchronously, the triggering signal to those heads which respond more quickly are delayed by the pulse generator to match the slowest-responding laser head. Only then can the wavefront sensing system time their gating accurately, adding $\sim 80\,\mu$s for propagation to 12 km height and back.

A 9530 series digital delay pulse generator from *Quantum Composers* triggers the three lasers of each side together. The signals of the fast photodiodes, which continuously measure the laser pulses, are read out by an *Agilent* DSO6014L oscilloscope. The output integrated in the ARGOS operating software as well as an interface to the pulse generator. Figure 7 demonstrates the successful delay compensation between the three lasers of one system's digital oscillogram, with lasers pulse width ranging roughly from 30 ns to 40 ns. The trigger timing delays of few microseconds are applied manually to the triggering signals of the laser heads with faster response, until the oscillogram confirms synchronicity.

4. SUMMARY AND OUTLOOK

The Laser Guide Star facility ARGOS is designed to provide the Large Binocular Telescope with Ground Layer Adaptive Optics correction over a wide field of view, to enhance the resolution and efficiency of the NIR camera and multi-object spectrographs LUCI. The twin laser systems each house three powerful 532 nm lasers, and optics to position the constellation of Rayleigh beacons to be projected on the sky. A broad range of diagnostics are implemented in the laser system off the primary beam paths, used for alignment, monitoring and flexure compensation.

Six commercial laser heads, with one additional spare, are the core component of the ARGOS facility. They underwent extensive testing during the past nine months which revealed several instances where heads fell short of

the power/beam quality requirements. The different causes were identified and resolved, and regular monitoring of each lasers performance during the coming months will confirm their reliability preceding commissioning.

A laboratory mock-up of one beam path was used as platform for early functionality and hardware–software interaction testing. As of date, the assembly and integration of components into the laser boxes is virtually complete. Both laser systems have been operated with the ARGOS software and their internal alignment is ongoing. One system and its electronic cabinets are presently installed on a telescope simulator where functionality of all components was confirmed. It is undergoing detailed full-system tests to verify the system specification requirements and a positive result is expected before the end of this summer.

ARGOS will be commissioned in stages, commencing with the laser system installation at the Large Binocular Telescope at the end of this year. The current progress looks promising for a successful first light at that time. The goal is to provide a well-aligned constellation and confirm operation in interaction with the LBT environment. The detailed characterization of the Ground-Layer Adaptive Optics facility performance will be evaluated at a later stage when the LGS dichroic and wavefront sensing unit are commissioned.

REFERENCES

[1] Rabien, S., Ageorges, N., Angel, R., Brusa, G., Brynnel, J., Busoni, L., Davies, R., Deysenroth, M., Esposito, S., Gässler, W., Genzel, R., Green, R., Haug, M., Lloyd Hart, M., Hölzl, G., Masciadri, E., Pogge, R., Quirrenbach, A., Rademacher, M., Rix, H. W., Salinari, P., Schwab, C., Stalcup, Jr., T., Storm, J., Strüder, L., Thiel, M., Weigelt, G., and Ziegleder, J., "The laser guide star program for the LBT," in [*Society of Photo-Optical Instrumentation Engineers (SPIE) Conference Series*], *Society of Photo-Optical Instrumentation Engineers (SPIE) Conference Series* **7015** (July 2008).

[2] Gaessler, W., Rabien, S., Esposito, S., Barl, L., Beckmann, U., Bluemchen, T., Bonaglia, M., Borelli, J., Brusa, G., Brynnel, J., Buschkamp, P., Busoni, L., Carbonaro, L., Connot, C., Davies, R., Deysenroth, M., Durney, O., Green, R., Hans, G., Gasho, V., Haug, M., Hubbard, P., Ihle, S., Kulas, M., Lederer, R., Lewis, J. E., Loose, C., Lehmitz, M., Noenickx, J., Nussbaum, E., Orban de Xivry, G., Peter, D., Quirrenbach, A., Rademacher, M., Raab, W., Rahmer, G., Storm, J., Schwab, C., Vaitheeswaran, V., and Ziegleder, J., "Status of the ARGOS Ground Layer Adaptive Optics system," in [*Society of Photo-Optical Instrumentation Engineers (SPIE) Conference Series*], *Society of Photo-Optical Instrumentation Engineers (SPIE) Conference Series* **This Volume** (2012).

[3] Seifert, W., Appenzeller, I., Baumeister, H., Bizenberger, P., Bomans, D., Dettmar, R.-J., Grimm, B., Herbst, T., Hofmann, R., Juette, M., Laun, W., Lehmitz, M., Lemke, R., Lenzen, R., Mandel, H., Polsterer, K., Rohloff, R.-R., Schuetze, A., Seltmann, A., Thatte, N. A., Weiser, P., and Xu, W., "LUCIFER: a Multi-Mode NIR Instrument for the LBT," in [*Society of Photo-Optical Instrumentation Engineers (SPIE) Conference Series*], Iye, M. and Moorwood, A. F. M., eds., *Society of Photo-Optical Instrumentation Engineers (SPIE) Conference Series* **4841**, 962–973 (Mar. 2003).

[4] Buschkamp, P., Seifert, W., Polsterer, K., Lehmitz, M., Lederer, R., Gemperlein, H., Naranjo, V., Ageorges, N., Hofmann, R., Eisenhauer, F., Rabien, S., Honsberg, M., and Genzel, R., "LUCI in the sky: performance and lessons learned in the first two years of near-infrared multi-object spectroscopy at the LBT," in [*Society of Photo-Optical Instrumentation Engineers (SPIE) Conference Series*], *Society of Photo-Optical Instrumentation Engineers (SPIE) Conference Series* **This Volume** (2012).

[5] Bonaglia, M., "Design of the wavefront sensor unit of ARGOS, the LBT laser guide star system," *ArXiv e-prints* (Mar. 2012).

[6] Busoni, L., Bonaglia, M., Esposito, S., Carbonaro, L., and Rabien, S., "Final design of the wavefront sensor unit for ARGOS, the LBT's LGS facility," in [*Society of Photo-Optical Instrumentation Engineers (SPIE) Conference Series*], *Society of Photo-Optical Instrumentation Engineers (SPIE) Conference Series* **7736** (July 2010).